Journal of the European Ceramic Society 15 (1995) 617–622

0955-2219(95)00023-2
0955-2219/95/$9.50

Problems Associated with Imaging Resistive Barriers in $BaTiO_3$ PTC Ceramics Using the SEM Conductive Mode

J. D. Russell[a]* & C. Leach[b]

[a]Department of Materials, Imperial College of Science, Technology and Medicine, London, SW7 2BP, UK
[b]Manchester Materials Science Centre, University of Manchester and UMIST, Manchester, M1 7HS, UK

(Received 11 October 1994; revised version received 27 January 1995; accepted 31 January 1995)

Abstract

The micro-electrical properties of $BaTiO_3$ have been studied using the remote electron beam induced current technique. Difficulties associated with applying this technique to low resistance, inhomogeneous ceramics are discussed and illustrated with the example of PTCR materials. At temperatures above the Curie temperature, contrast steps corresponding to resistive interfaces are observed with differing sensitivities according to the imaging conditions used. The image noise decreases and the current sensitivity increases with the sample resistance. Remote electron beam induced current contrast in $BaTiO_3$, showing the high resistivity transition does not occur uniformly as a function of temperature across all grain boundaries.

Introduction

Semiconducting barium titanate and related phases are important electroceramic materials which have been used for their positive temperature coefficient (PTC) of resistance properties in applications such as over-temperature protection and current limiting devices for over thirty years,[1] and are still very important technologically.[2] The most widely accepted model of the PTC effect, due to Heywang,[3] is of back to back Schottky barriers at grain boundaries due to a build up of negative interface charge. This gives rise to a potential barrier whose height depends on the dielectric constant. Since the dielectric constant changes abruptly at the phase transformation, the barrier height and resistivity change accordingly. This model was extended by Jonker who also considered ferroelectric effects below T_c, where spontaneous polarisation reduces the expected potential barrier height.[4]

However, while the gross behaviour is well explained by these models, sensitive structure averaging techniques such as impedance measurements reveal that they do have some shortcomings.[5–7] The introduction of modified models, such as that of Daniels and Wernicke[8] have caused a parallel search for explanations of the PTC effect at the grain level due to the strong effect of heterogeneity on the electrical properties.[9] TEM investigations clearly show the ferroelectric domains below T_c and also that there is no intergranular phase present of width greater than 2–10 nm.[10] Cathodoluminescence microscopy has been used to observe grain boundary potential barriers in PTC material.[11] EBIC has also been used to view the domains and grain boundaries.[12] However, none of these studies offered direct observation of the resistive properties of such materials.

In this paper we discuss the practicalities of the application of a little used variant of the EBIC technique which allows direct observation of the resistivity changes of individual grain boundaries as the resistive transition progresses, allowing detailed determination of device homogeneity.

EBIC Phenomenology in Ceramics

The well-known charge collection imaging mode of the scanning electron microscope (SEM) is often applied to the microcharacterisation of semiconductors. In this mode the impinging electron beam generates a multitude of electron–hole pairs which can then be separated by built-in fields such as those at pn-junctions. By using a suitable contact geometry, charge collection currents several orders of magnitude larger than the beam current

*Now at Manchester Materials Science Centre, University of Manchester and UMIST, Manchester, M1 7HS, UK

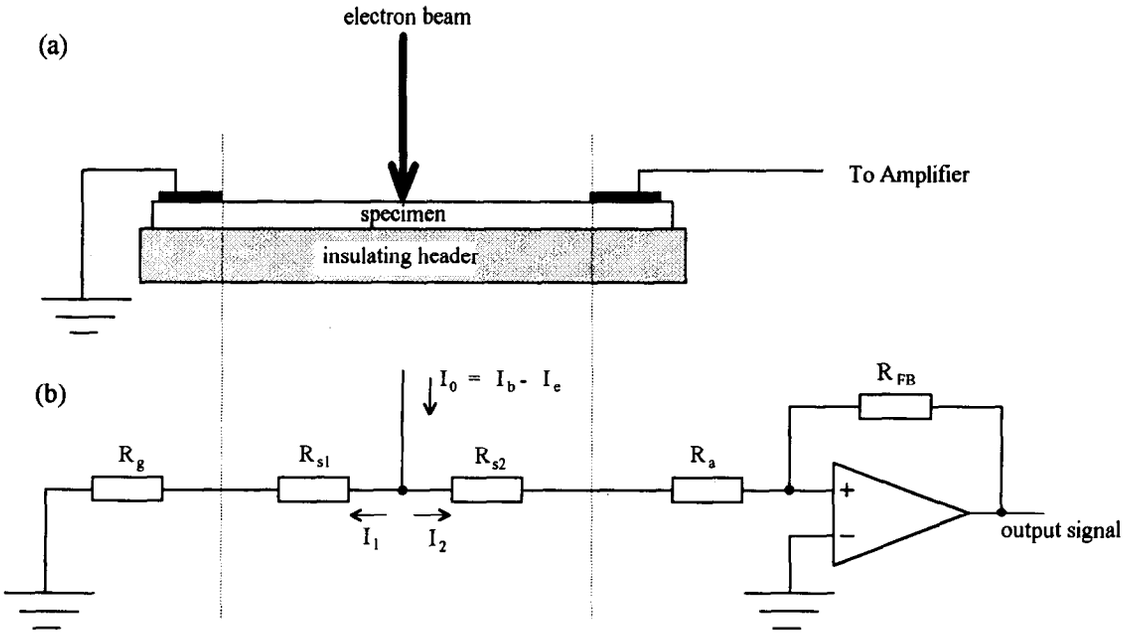

Fig. 1. (a) Specimen configuration and (b) equivalent circuit for REBIC mode imaging. R_g is the resistance from the left of the sample to earth, R_a is from the right of the sample to the amplifier input, I_b is the beam current, I_e the total emitted current, R_{s1} and R_{s2} are the specimen resistances to the left and right contacts from the beam impact point, and $R_{s1} + R_{s2} = R_s$, the specimen resistance. The amplifier is shown schematically, with feedback resistance RFB.

can be obtained in a technique called electron beam induced current (EBIC).[13] In the case of less-well characterised materials such as electroceramics, the absence of suitable built-in fields, and much larger recombination centre densities mean that the usual charge collection mode geometries do not always work as effectively, or at all. However, a technique first used by Matare and Laakso[14] and subsequently termed remote electron beam induced current (REBIC) by Bubulac and Tennant[15] can be employed.

If the specimen has two closely separated contacts as shown in Fig. 1(a), it will have an equivalent circuit as shown in (b), where R_g represents all resistances between the scanned region of the inter-electrode observation area and earth via the earth electrode, and R_a all resistances between the scanned area and earth via the amplifier. R_{s1} and R_{s2} are the components of the scanned area resistance (total R_s) immediately to the left and to the right of the impinging beam. The specimen acts as a current divider with the net current injected by the electron beam flowing either directly to earth through the left contact or to the right through the low input impedance current amplifier. The proportion of I_b reaching the amplifier is used to modulate the signal on the viewing screen and results in a contrast gradient. In some ceramics, electrically active regions cause charge collection contrast due to separated electron–hole pairs. Such contrast would be superimposed on the resistive baseline,[16] and has been observed in ZnO varistor material, for example,[17] where the presence of grain boundary barriers can be satisfactorily explained by grain boundary EBIC models.[18] However, frequently such contrast is not seen and only effects due to the passive resistance component of the interfaces are observed. In this case the imaging method can be referred to as resistive contrast imaging (RCI).[19]

The RCI quality is affected by four factors, as described below.

Current sensitivity

If we consider the case when the scanned area is the total width of sample between the contacts, it can simply be shown, using the terminology of Fig. 1 that the currents which flow through the amplifier when the beam impinges on the sample adjacent first to the left and then the right contact are given by

$$I_{left} = I_o \frac{R_g}{R_g + R_s + R_a} \quad (1)$$

$$I_{right} = I_o \frac{R_g + R_s}{R_g + R_s + R_a} \quad (2)$$

In the case of $BaTiO_3$ the sample resistance, R_s varies widely with temperature, which causes the imaging characteristics to vary. We can define a quantity called the current sensitivity, S,

$$S = \frac{I_{right} + I_{left}}{I_b} \quad (3)$$

where I_b is the beam current. The current sensitivity describes the possible current variation, and hence

contrast, across the sample as a fraction of the beam current, and must be larger than the noise floor for meaningful images to be observed. Although the noise generated by a typical amplifier may only be of the order of picoamperes, as will be seen later, the observed noise can be affected greatly by the sample resistance. It is thus often necessary to work with beam currents of several nA and larger which in turn limits the spatial resolution. The effect of noise is much more important than in charge collection imaging of semiconductors, in which charge multiplication causes a gain of about 1000 over the beam current level. In contrast, RCI of electrical ceramics leads to signals of the order of the beam current. In the case of $BaTiO_3$ PTCR material, a typical sample mounted in the SEM may vary in resistance from 30Ω below the Curie temperature to 30 kΩ above it. From eqns (1–3), using $R_g \approx 10\Omega$, $R_a = 40\Omega$ and $I_o/I_b \approx 0{\cdot}8$ this gives S values of 0·3 and 0·8. Thus the current sensitivity is changed by a factor of 2·7, as is the image contrast, on crossing the phase transition.

Geometrical effects

For a given specimen the largest current sensitivity, and hence the largest current contrast, will be seen if the electrodes are at the image edges. If the field of view spans only part of the electrode separation, the current resolution will be reduced proportionately, i.e. neglecting contact resistances

$$S' = S\frac{w}{D} \tag{4}$$

where w is the image field-width and D the inter-electrode spacing. Thus it is important in detailed work to locate the electrodes as close together as possible. Unfortunately this configuration limits flexibility in aereal imaging and reduces the overall resistance of the sample which gives rise to further difficulties as described in the next section.

Amplifier limitations

For specimen resistances which are small compared with the input impedance of the detecting amplifier, both amplifier noise and the input offset voltage which appear at the inputs of the operational amplifier are magnified in effect. The equation describing the noise amplification is of the form

$$V_{\text{output noise}} = V_{\text{input noise}}\left(1 + \frac{R_{FB}}{R_g + R_s + R_a}\right) \tag{5}$$

where R_s is the sample resistance and R_{FB} is the amplifier feedback resistance (Fig. 1(b)). The value of R_{FB} fixes the amplifier gain, and a typical value for R_{FB} under our experimental conditions would be 100 MΩ. Thus, for the case of the PTCR described previously, the output noise increases by a factor of 1000 in the low temperature, low resistance state compared with its high temperature variant. A similar relationship exists for the amplifier input offset voltage which changes as the sample resistance changes. Although the latter can, in principle, be corrected by applying an appropriate back-off current, in practice for PTCR materials undergoing the phase transformation, the steepness of the change of resistance with temperature means that the signal drifts over a large range with small variations in the sample temperature leading to excessive signal instability.

One way to circumvent this is to add a resistor in series with the sample which will reduce the noise and signal instability. Additionally, this will decrease the total current sensitivity by making the specimen a smaller part of the overall current divider circuit. For example, whilst reducing the noise substantially, adding a 1 kΩ resistor would change the current sensitivity values from 0·3 and 0·8 to 0·022 and 0·77 using the sample resistance values previously cited. It is thus possible to extend downwards the range of sample resistances for which useful images can be obtained. However, because of the close interdependence of the noise and sensitivity, the optimal resistance value required is usually a compromise.

Backscattering contrast effects

On average, around 20% of the beam current is lost from the sample by re-emission as backscattered or secondary electrons. The RCI current will be reduced in regions where a large proportion of the incident beam current is lost. Grains with different backscattering coefficients will, as a consequence, show different contrast in the RCI image for which a correction must be made. This can in principle be achieved by taking a specimen current image (by removing the earth contact so that all the absorbed current must flow to earth through the amplifier) and using it to adjust the measured RCI signal intensity at each point according to

$$I_R = \frac{I'_R}{I_s} \tag{6}$$

where I_R and I_R' are the true and measured RCI currents respectively, and I_s is the local specimen current. Such corrections are small for materials which are predominantly single phase.

Experimental

Polished samples with a 3 mm electrode spacing were prepared from a commercial PTC thermistor device with a Curie temperature of 80°C. These

specimens were mounted on an Oxford Instruments H1001 heating stage, and electrical connections were made using a micromanipulator with fine tungsten probes. A Matelect ISM5 EBIC amplifier was used to amplify the input signal for the SEM.

Subsequently the current sensitivity was increased for higher magnification imaging by reducing the contact separation. This was achieved by producing an array of closely spaced ohmic contacts on the sample surface by careful cleaning and evaporation of aluminium onto a polished sample using a fine TEM grid as a mask.

Results and Discussion

Fig. 2(a) is an RCI image of a region of the polished sample taken with the sample heated to well above the Curie temperature. The inter-electrode spacing is approximately 3 mm left–right in the image. The contrast gradient from left to right is clearly visible, as are the resistive interfaces where abrupt steps in the signal occur. The width of the steps is much larger than the grain size and so at this sensitivity we see clusters of grains of similar grey-level bounded by interfaces with intensity steps. This effect is sometimes referred to as terrace contrast.

As the imaging temperature is decreased, the substantial decrease in sample resistance results in the image becoming more noisy as predicted, along with a parallel decrease in the current sensitivity. However, once this decrease in current sensitivity (Fig. 2(b)), is corrected for, the terraced microstructure can be seen to persist to quite low temperatures until it is lost ultimately in the noise floor. It is thus not clear whether the terraced structure disappears altogether at lower temperatures, or it is simply beyond the capabilities of the imaging technique to observe it. Thus the terrace structure imaged in this way is not necessarily related to the PTCR effect, but may be linked to some intrinsic microstructural feature, such as relics of powder agglomeration prior to sintering.[20] It can be seen from Fig. 2(c) that on increasing the magnification, using this specimen configuration little extra information is seen; contrast is poor with effects only visible at some interfaces. This is due to the lack of current sensitivity when observing a small region between widely spaced contacts (see eqn (4)).

Figure 3 shows the results of a further examination of the same material at higher magnification and higher current sensitivity. This was achieved by using more closely spaced contacts as previously described. A sequence of reproducible

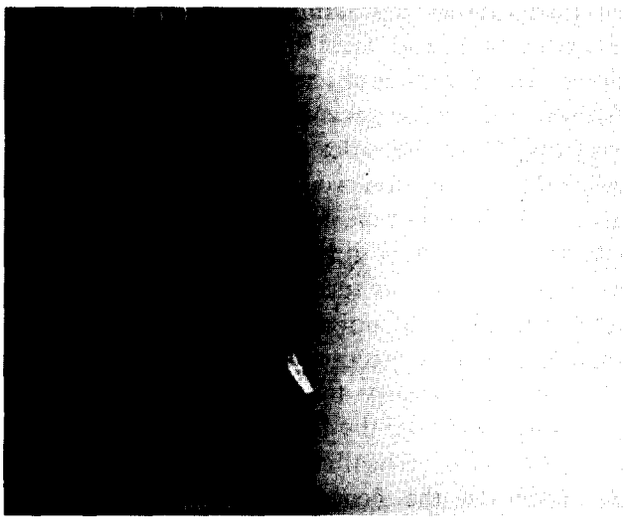

(a)

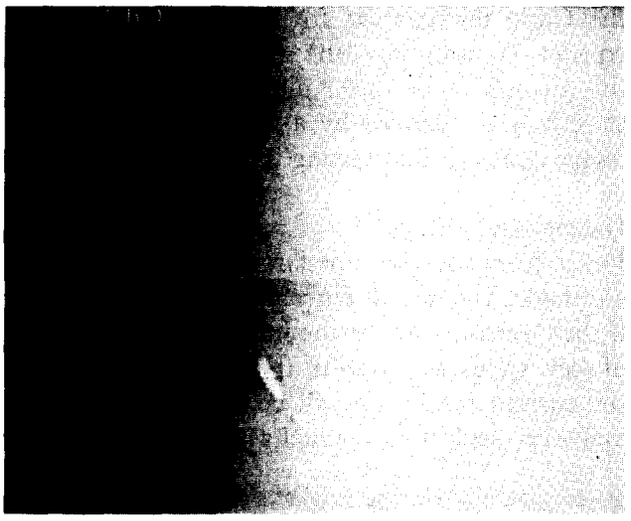

(b)

(c)

Fig. 2. (a) RCI image between widely separated contacts on $BaTiO_3$ at 140°C showing terrace contrast. (b) is the same area at 110°C where the contrast of the lower half of the image has been scaled to allow for the decreased current sensitivity. The image also shows the increased noise associated with the lower sample resistance. (c) is a higher magnification image of a region from (a). Scale bar (a) and (b) = 100 μm, (c) = 10 μm.

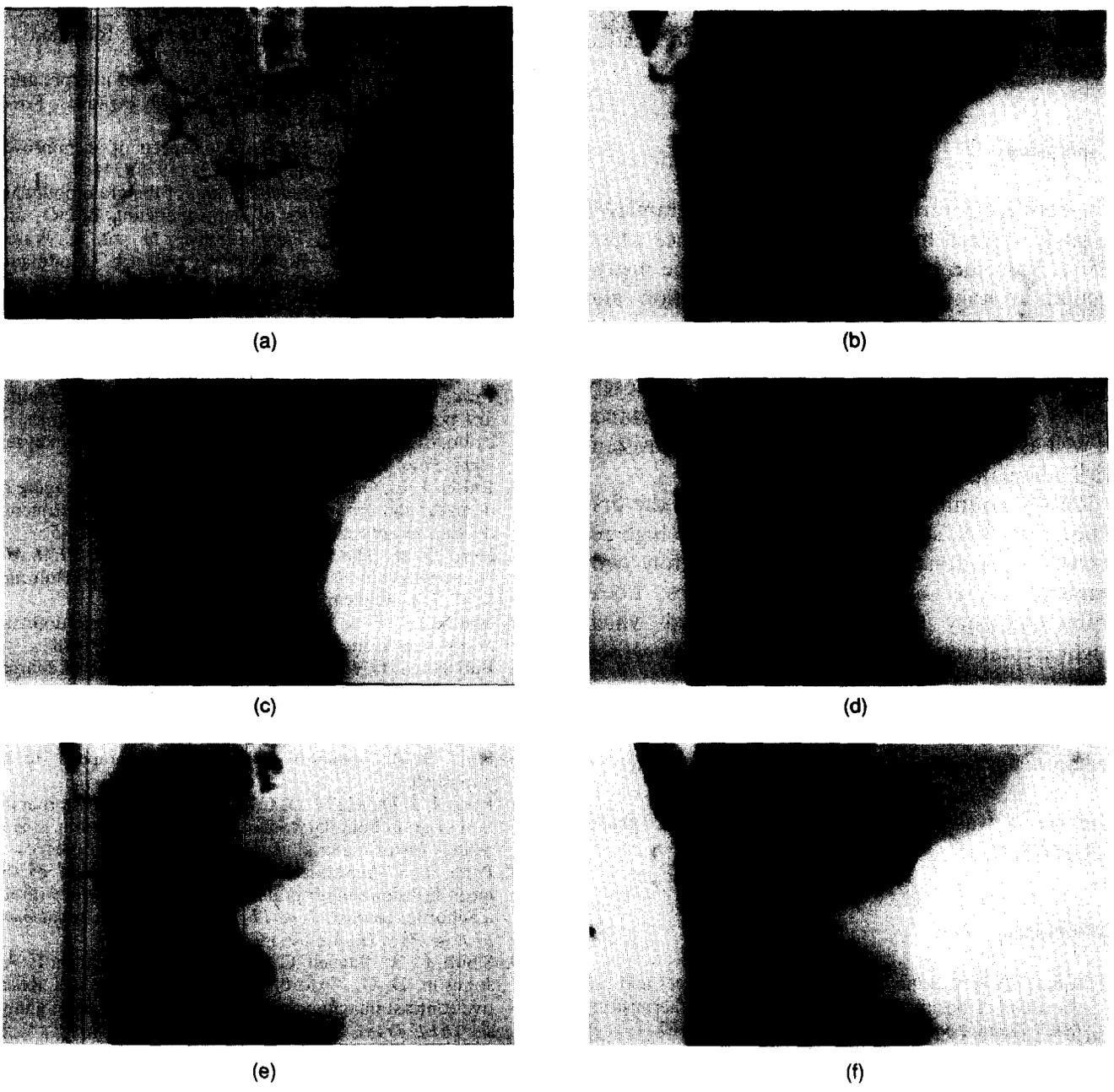

Fig. 3. (a) Secondary electron image showing the grain structure, with the contacts labelled 'L' and 'R'. The left contact is partially covered by a probe. (b–f) are a series of resistive contrast images at 110, 120, 130 and 140°C respectively. In (f) 'A' is an example of a resistive barrier, while 'B' denotes extended regions surrounding grain boundaries also visible in the other images. Scale bar = 10 μm.

images taken in the temperature range 110°C–140°C, where the PTCR effect is active is shown. Figure 3(a) is the corresponding secondary electron image, showing the grain structure and the positions of the two contacts 'L' and 'R', of which the former is covered by one of the micromanipulator probes. Several features are evident.

The REBIC images in Fig. 3(b–f) show that as the temperature increases the image becomes less noisy, and the contrast gets stronger, in accordance with the earlier discussion. This is most clearly evident by comparing (b) and (f).

Each grain boundary that increases its resistance leads to a new contrast step (such as that labelled 'A' Fig. 3(f)) between the contact pads and a slight readjustment of the overall intensity gradient, which is always from approximately left to right. In the later images of the Fig. 3(b–f), more high resistance grain boundaries are introduced compared with the earlier micrographs. It is clearly seen that different barriers become highly resistive at different temperatures, as evidenced by the change in the steps of the contrast profile across the centre of the images with increasing temperature.

Extended regions bounded by resistive barriers spanning grain boundaries occur on the two vertical grain boundaries at the bottom of each image (labelled 'B' in Fig. 3(f)). Backscattered channelling pattern analysis showed that these regions are not crystallographically distinct. Their origin is

unclear, but they might be related to broad impurity diffusion zones as observed in related materials.[21,22]

Conclusions

The resistive contrast shown by electroceramics is strongly affected by the specimen resistance which affects both the current sensitivity and the instrumentation noise. The electrode separation and backscattered electron current loss also need to be taken into consideration. Imaging conditions can be optimised by using specially fabricated, closely spaced electrodes and additional series resistance as well as using the largest beam current consistent with adequate spatial resolution.

REBIC contrast has been observed for the first time in $BaTiO_3$, showing directly that the high resistivity transition does not occur uniformly with temperature across all grain boundaries. Local grain boundary features were observed which might (tentatively) be attributable to a delocalised impurity diffusion phenomenon.

Acknowledgements

This work was carried out under EPSRC grant GR/946783.

References

1. Saburi, O. & Wakino, K., Processing techniques and applications of positive temperature coefficient thermistors. *IEEE Trans. Compon. Parts*, **CP-10** (1963) 53–67.
2. Kulwicki, B. M., Trends in PTC resistor technology. *SAMPE Journal*, **23**(6) (1987) 34–8.
3. Heywang, W., Resistivity anomaly in doped barium titanate. *J. Am. Ceram. Soc.*, **47** (1964) 484–90.
4. Jonker, G. H., Some aspects of semiconducting barium titanate. *Sol. State Electron.*, **7** (1964) 895–903.
5. Sinclair, D. C. & West, A. R., Bulk PTC effect on doped $BaTiO_3$. *J. Mater. Lett.*, **7** (1988) 823–4.
6. Sundaram, S. K., Complex-plane impedance analysis of PTC thermistor–intergranular capacitor transition. *J. Appl. Phys. D: Appl. Phys.*, **23** (1990) 103–7.
7. Michenaud, J.-P. & Gillot, C., About the interpretation of the PTC effect in Nb-doped $BaTiO_3$ ceramics. *Ferroelectrics*, **127** (1992) 41–6.
8. Daniels, J. & Wernicke, R. New aspects of an improved PTC model. *Philips Res. Repts.*, **31** (1976) 544–9.
9. Abelard, P., Present understanding of the grain boundary electrical characteristics of semiconducting $BaTiO_3$ and $SrTiO_3$ ceramics, in *Electroceramics IV*. ed. R. Waser, S. Hoffmann, D. Bonnenberg and Ch. Hoffmann. Augustinus Buchhandlung, Aachen, Germany, 1994, pp. 541–8.
10. Haanstra, H. B. & Ihrig, H., Transmission electron microscopy at grain boundaries of PTC-type $BaTiO_3$ ceramics. *J. Am. Ceram. Soc.*, **63** (1980) 288–91.
11. Ihrig, H. & Klerk, M., Visualization of the grain boundary potential barriers of PTC-type $BaTiO_3$ ceramics by cathodoluminescence in an electron-probe microanalyzer. *Appl. Phys. Lett.*, **35** (1979) 307–9.
12. Ralph, J. E., Gowers, J. P. & Burgess, M. R., Imaging of domains and grain boundaries in a ferroelectric semiconducting ceramic. *Appl. Phys. Lett.*, **41** (1982) 343–5.
13. Holt, D. B., The Conductive Mode. Ch 6 in *SEM Microcharacterisation of Semiconductors*. ed. D. B. Holt and D. C. Joy. Academic Press, London, 1989.
14. Matare, H. F. & Laakso, C. W., Space-charge domains at dislocation sites. *J. Appl. Phys.*, **40** (1969) 476–82.
15. Bubulac, L. O. & Tennant, W. E., Observation of charge-separating defects in HgCdTe using remote contact electron-beam induced current. *Appl. Phys. Lett.*, **52** (1988) 1255–7.
16. Holt, D. B., Insulator EBIC: Basic Phenomena, to be published.
17. Russell, J. D., Halls, D. C. & Leach, C., Direct observation of grain boundary Schottky barrier behaviour in zinc oxide varistor material. *J. Mater Sci. Lett.*, (in press).
18. Palm, J. & Alexander, H., Direct measurement of the local diffusion length grain boundaries by EBIC without a Schottky contact. *J. de Phys IV, Colloq. C6, supplement to J. de Phys III*, **1** (1991) C6-101–6:
19. Smith, C. A., Bagnell, C. R., Cole, E. I., Dibianca, F. A., Johnson, D. G., Oxford, W. V. & Propst, R. H., Resistive contrast imaging: a new SEM mode for failure analysis. *IEEE Trans. El. Dev.*, **ED-33** (1986) 282–4.
20. Halls, D. C. & Leach, C., Processing induced resistive barriers in ZnO material. Submitted to *J. Mater. Sci.*,
21. Hennings, D. & Rosenstein, G., Temperature-stable dielectrics based on chemically inhomogeneous $BaTiO_3$. *J. Am. Ceram. Soc.*, **67** (1984) 249–54.
22. Al-Saffer, R., Azough, F. & Freer, R., A STEM study of core-shell structures in an x7r-type ceramic. *IOP Conf. Ser.* No. 130 (1993) pp. 379–82.